

# Human-Robot Interface to Operate Robotic Systems via Muscle Synergy-Based Kinodynamic Information Transfer\*

Janghyeon Kim<sup>1</sup>, Dae Han Sim<sup>1</sup>, Ho-Jin Jung<sup>1</sup>, Ji-Hyeon Yoo<sup>1</sup>, Changjae Lee<sup>1</sup>, and Han Ul Yoon<sup>2</sup>

**Abstract**—When a human performs a given specific task, it has been known that the central nervous system controls modularized muscle group, which is called muscle synergy. For human-robot interface design problem, therefore, the muscle synergy can be utilized to reduce the dimensionality of control signal as well as the complexity of classifying human posture and motion. In this paper, we propose an approach to design a human-robot interface which enables a human operator to transfer a kinodynamic control command to robotic systems. A key feature of the proposed approach is that the muscle synergy and corresponding activation curve are employed to calculate a force generated by a tool at the robot end effector. A test bed for experiments consisted of two armband type surface electromyography sensors, an RGB-d camera, and a Kinova Gen2 robotic manipulator to verify the proposed approach. The result showed that both force and position commands could be successfully transferred to the robotic manipulator via our muscle synergy-based kinodynamic interface.

## I. INTRODUCTION

In 1967, Bernstein found that modularized muscle groups were coactivated by the central nervous system when people performed a specific task[1]. For last two decades, studies have found the existence of the modularized muscle group for various tasks, e.g., balance maintenance[2], swimming[3], reaching movements by hands[4], grasping and picking an object[5], and so on. The modularized muscle group is called “muscle synergy”[6], [7], [8]. The muscle synergy can be extracted from surface electromyography (sEMG) by using non-negative matrix factorization[9].

The muscle synergy can serve as a useful tool for human-robot interface design due to their characteristics, i.e., modularized and predetermined for a specific task. Günay et al. employed muscle synergy for hand posture classification; especially, a grasp classification for activities in daily living[10]. Furui et al. developed an impedance model-based biomimetic prosthesis control by utilizing the muscle synergy as motion primitives to determine combined motions[5]. Those two research exemplify that the muscle synergy can contribute to reduce the dimensionality of control signal as well as the complexity of classification problem to

identify various posture and motions, which are essential for human-robot interface design.

The interpretation of muscle synergy also gives us an information about the direction and magnitude of limb movement. Berger and d’Avella presented a method to translate a muscle synergy into a force in two dimensional Cartesian space[4], and Camardella et al. proposed an approach to map a muscle synergy onto a force[11]. Chen et al. showed that the activation curve of a muscle synergy can be used to calculate a force generated by a hand[12]. All these existing findings substantiate that we can obtain a force-related information about a specific movement by analyzing the muscle synergy and corresponding activation curve.

This paper proposes a human-robot interface design approach to operate robotic systems via kinodynamic information transfer. Specifically, both joint-and-skeleton and sEMG data are measured by RGB-d camera and armband type EMG sensor, respectively, while a pilot user is performing a specific task and then utilized to manipulate a robotic system with force and position commands. A key feature of our proposed design approach is that muscle synergies and corresponding activation curves are interpreted to determine the force command. To our best knowledge, the human-robot interfaces via muscle synergy-based kinodynamic transfer have not been fully considered; therefore, findings from this study can contribute to the state of the arts in a field of the human-robot interface design.

The rest of the paper is organized as follows: the proposed methodology to calculate muscle synergy-based kinodynamic information is introduced in Section 2. Specifically, our approach to obtain force and position command will be explained. In Section 3, the experimental test bed to verify the proposed approach is presented. The results are reported and significant outcomes are discussed in Section 4. Section 5 will be the conclusion of this paper.

## II. METHODS

### A. Muscle Synergy: Definition

Let  $M \in \mathbb{R}^{d \times k}$  be  $d$ -channel sEMG signal for a time step  $k$ . Also, let a column vector  $w_i = [w_{i1}, w_{i2}, \dots, w_{id}]^T \in \mathbb{R}^{d \times 1}$  be an  $i^{\text{th}}$  muscle synergy which is a modularized muscle group consisting of the contribution of each muscle. A row vector  $c_i = [c_{i1}, c_{i2}, \dots, c_{ik}] \in \mathbb{R}^{1 \times k}$  denotes the corresponding activation curve of the muscle synergy  $w_i$ . Figure 1 shows an illustrative example of the muscle synergy in case of the number of channels and synergies are  $d = 3$  and  $n = 2$ , respectively. Consequently,  $M$  can be expressed

\*This work was primarily supported by the National Research Foundation of Korea(NRF) grant funded by the Korea government (MSIT) (Grant No. 2021R1F1A1063339) and partially supported by the MSIT National Program for “Excellence in SW (Grant No. 2019-0-01219)” supervised by the Institute of Information and communications Technology Planning and evaluation (IITP).

<sup>1</sup>Janghyeon Kim, Dae Han Sim, Ho-Jin Jung, Ji-Hyeon Yoo, Changjae Lee are with the Department of Computer Science, Yonsei University (Mirae), Wonju, Gangwon 26493, Korea {janghyeonk, dhsim, ho-jin.j, jihyeonyoo, cjlee7128}@yonsei.ac.kr

<sup>2</sup>Han Ul Yoon is with Faculty of the Division of Software, Yonsei University (Mirae), Wonju, Gangwon 26493, Korea huyoon@yonsei.ac.kr

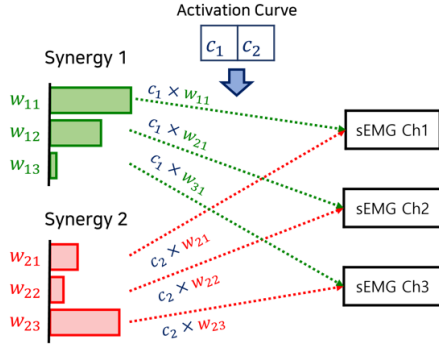


Fig. 1. An illustrative example of the muscle synergy in case of the numbers of channels and synergies are  $d = 3$  and  $n = 2$ , respectively.

as follows:

$$M = \sum_{i=1}^n w_i \times c_i. \quad (1)$$

$w_i$  and  $c_i$  can be found by applying the non-negative matrix factorization algorithm presented in [9].

### B. Obtaining the Muscle Synergy-Based Kinodynamic Information

Procedure to obtain the muscle synergy-based kinodynamic information, i.e., the force and position commands for robotic systems, consists of the following three steps:

- 1) Find a muscle synergy of which mostly correlated to human generated force.
- 2) Calculate a force generated by a tool at the robot end effector.
- 3) For position command, use the vector flow of the human operator hand's joint-and-skeleton data.

First, let  $F_h \in \mathbb{R}^{1 \times k}$  be the magnitude of a force generated by a human operator for time step  $k$  while performing a given specific task; for instance, the human operator is instructed to press down a solid surface with a tool in his hand. Recall that  $w_i$  and  $c_i$  represent a muscle synergy and a corresponding activation curve, respectively. Since  $c_i$  is proportionally related to  $F_h$ , we can find the muscle synergy of which mostly correlated to the given specific task, denoted by  $w_{F_h}$ ,

$$\arg \max_i \{F_h c_i^T\} \text{ then } w_{F_h} \equiv w_i, \quad (2)$$

and the corresponding activation curve can be determined straightforwardly as  $c_{F_h} \equiv c_i$ .

Next, let  $\hat{F}$  represents the magnitude of force to be transferred to a robotic system, which the human operator wants to generate eventually by a tool at the robot end effector.  $\hat{F}$  can be calculated by

$$\hat{F} = \alpha c_{F_h} \quad (3)$$

where  $\alpha$  is a positive constant. We note that similar approaches can also be found in [11], [12].

Lastly, the vector flow of the human operator hand's joint-and-skeleton data, which can be obtained by RGB-d camera, is directly used for position command.

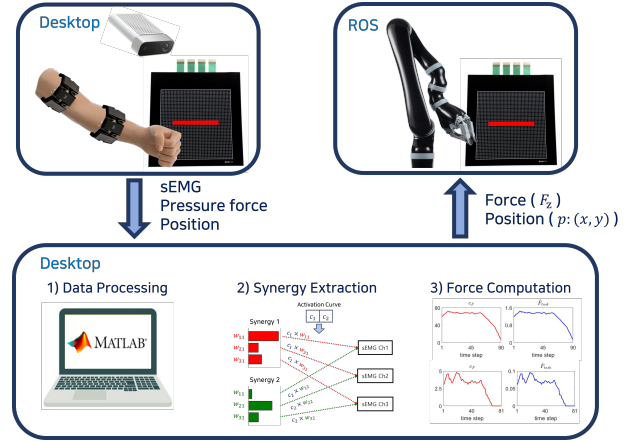


Fig. 2. The system architecture of the proposed human-robot interface for kinodynamic information transfer.

Figure 2 presents the system architecture of the proposed human-robot interface.

## III. EXPERIMENTS

### A. Pilot human operator and Given Task

A pilot human operator was equipped with two armband type sEMG sensors on his upper arm and forearm, respectively. For each sEMG sensor, the channel deployment of the two sEMG sensors is summarized in Table I. The pilot human operator was instructed to grip a digital pencil and draw a line from the left to the right five times by pressing a solid surface with two different force strengths: weak and strong; Hence, the pilot human operator drew a line for 10 trials.

TABLE I  
THE CHANNEL DEPLOYMENT OF THE TWO SEMG SENSORS

	Ch #1, #2, #3	Ch #5, #6, #7	Ch #4, #8
Upper Arm	Bicep Area	Tricep Area	Boundary b/w channels
Forearm	Radius Side	Ulna Side	Boundary b/w channels

### B. Data Collection and Processing

While the pilot human operator was performing the given task, sEMG data, the position of an index finger, and pressure force were measured by the two armband type sEMG sensors (MyoArmband, Tahlmic Labs, Brooklyn, NY), an RGB-d camera (Kinect Azure, Microsoft, Redmond, WA), and a pressure mat (MS9717, Kitronyx, Seoul, Republic of Korea), respectively. The  $z$ -axis of the RGB-d camera was aligned to the surface norm direction of the pressure mat. Under the pilot human operators demonstration, the robotic manipulator (Kinova Gen2+KG3, Kinova, Quebec, Canada) drew a line on  $xy$ -plane.

The data processing was performed as follows. First, the sEMG data was moving average filtered, the pressure force was calculated by summing up all returned value from  $16 \times 10$

cells, and the position of the index finger was recorded and the Kalman filter was applied. Next, after filtering processes, all data were up/down sampled to make them of the same length. Lastly, by following the presented approach in [13], all data during 10 trials were concatenated. Consequently, we have

- $M$ : sEMG data  $\mathbb{R}^{16 \times 939}$ . The 1<sup>st</sup>(9<sup>th</sup>) through 8<sup>th</sup>(16<sup>th</sup>) row data corresponds to upper arm(forearm).
- $F_h$ : the force generated by the pilot human operator  $\mathbb{R}^{1 \times 939}$ .
- $p$ : the  $(x, y)$  position of the index finger  $\mathbb{R}^{2 \times 939}$ .

### C. Muscle Synergy Extraction and Kinodynamic Information Calculation

To calculate a force command  $\hat{F}$ , muscle synergies were extracted from  $M \in \mathbb{R}^{16 \times 939}$  under 90% variation accounted for (VAF) [9], [8]. From the extracted  $w_i \in \mathbb{R}^{16 \times 1}$  and  $c_i \in \mathbb{R}^{1 \times 939}$ , we could find  $w_{f_h}$  by (2). Afterward,  $\hat{F}$  was calculated by (3).  $\alpha$  was set to 20. To distinguish two different pressure forces demonstrated by a pilot human operator,  $\hat{F}_{\text{weak}}$  and  $\hat{F}_{\text{strong}}$  will be used in Section IV.

As aforementioned, the position command  $p$  could be directly obtained from RGB-d camera data. Finally, the force generated by a tool at the robot end effector, denoted by  $F_r$ , was measured by the pressure mat.  $F_h$  and  $F_r$  were analyzed and compared each other.

## IV. RESULTS

### A. Result 1: Extracted Muscle Synergies and Force Command

Figure 3 show the extracted muscle synergies (top row) and the corresponding activation curves (bottom row) from the concatenated 10 trials sEMG data under the number of synergies  $n = 3$ . From the extracted muscle synergies, the size of bar graph represents the contribution of individual muscle for each synergy. The first half of the activation curves along time step shows the activation of the corresponding muscle synergy while a pilot user is drawing a line with weak pressing force whereas the second half presents the activation under a strong pressing force. Both the muscle synergies and the corresponding activation curves are inter-channel normalized.

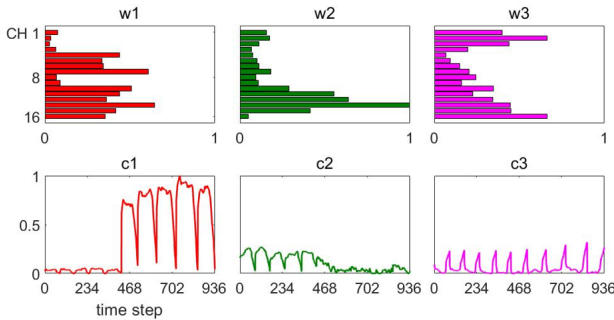


Fig. 3. The extracted muscle synergies (top row) and the corresponding activation curves (bottom row) from the concatenated 10 trials sEMG data ( $n = 3$ ).

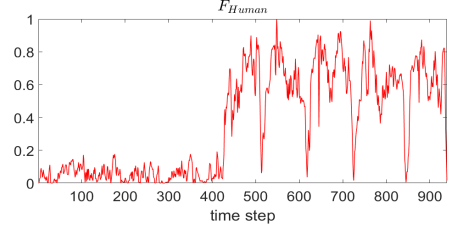


Fig. 4.  $F_h$  during a line drawing with a weak pressing force followed by a strong pressing force.

Figure 4 shows  $F_h$  during a line drawing with a weak pressing force followed by a strong pressing force. By using (2), we could find that  $w_{F_h} = w_1$  and accordingly  $c_{F_h} = c_1$ . We note that this result can be also observed by comparing  $c_i$ s in Fig. 3 to  $F_h$  in Fig. 4.

### B. Result 2: Operating Kinova Gen2 Robotic Manipulator via Kinodynamic Information Transfer

Figure 5 depicts the force commands  $\hat{F}_{\text{strong}}$  and  $\hat{F}_{\text{weak}}$  for one trial which could be calculated using (3). We can see that  $\hat{F}_{\text{strong}}$  is ranging within  $[0.0, 1.5]$  whereas  $\hat{F}_{\text{weak}}$  has values within  $[0.0, 0.1]$ . From Fig. 5, we could verify that  $\hat{F}_{\text{strong}}$  and  $\hat{F}_{\text{weak}}$  were successfully obtained for  $F_h$  of different pressing force.

Figure 6 shows the comparison result of  $F_h$  and  $F_r$  for one trial when  $\hat{F}_{\text{strong}}$  and  $\hat{F}_{\text{weak}}$  were transferred to the robotic manipulator, respectively. As shown in the Fig. 6, the gain of the transferred force command could be adjusted by  $\hat{F}_{\text{strong}}$  and  $\hat{F}_{\text{weak}}$ . It turned out that  $\alpha = 20$  in (3) was somewhat over-suppressed value for the force command transfer. We note that  $\alpha$  was set to 20 to guarantee a safe force-operation range for our robotic manipulator.

The comparison result of  $F_r$  under  $\hat{F}_{\text{strong}}$  and  $\hat{F}_{\text{weak}}$  is presented in Fig. 7. From Fig. 7, we can also check that muscle synergy-based kinodynamic information was successfully transferred and enabled us to operate the robotic manipulator with generating different force by the tool at the end effector.

Figure 8 shows the robot manipulator end-effector and human demonstrated trajectories on  $xy$ -plane. From Fig. 8, we can see that the human demonstration was well-transferred to the robotic manipulator end-effector, which substantiated kinematic information was successfully transferred via the proposed human-robot interface.

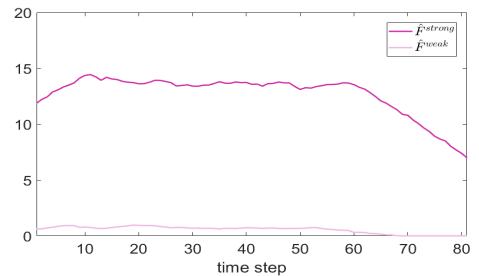


Fig. 5. The force command  $\hat{F}_{\text{weak}}$  and  $\hat{F}_{\text{strong}}$ .

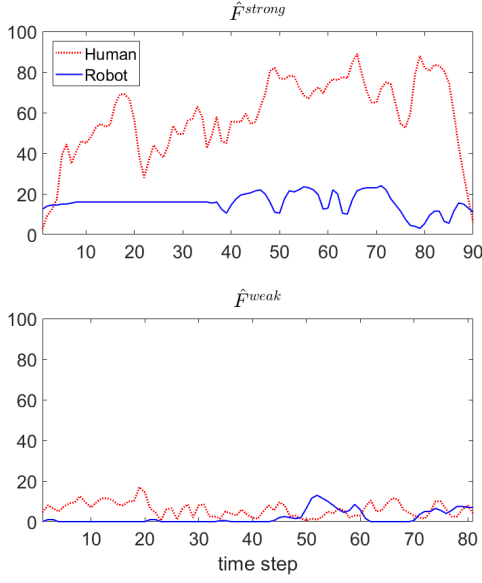


Fig. 6. The comparison result of  $F_h$  and  $F_r$  for one trial when  $\hat{F}_{strong}$  and  $\hat{F}_{weak}$  were transferred to the robotic manipulator.

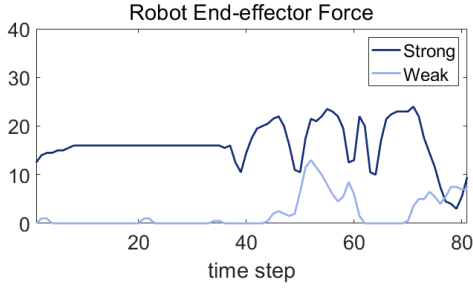


Fig. 7. The comparison result of  $F_r$  under  $\hat{F}_{strong}$  and  $\hat{F}_{weak}$ .

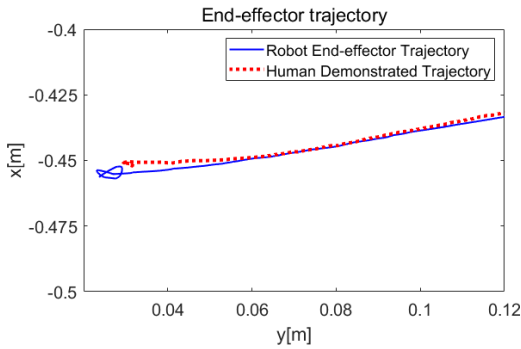


Fig. 8. Robot manipulator end-effector and human demonstrated trajectories on  $xy$ -plane.

## V. CONCLUSIONS

Throughout this paper, we proposed an approach to design a human-robot interface to operate robotic systems via muscle synergy-based kinodynamic information transfer. First, in our interface design, a pilot human operator's both kinematic data

and sEMG data were measured by armband type sEMG sensor and RGB-d camera, respectively. Next, muscle synergies were extracted from the measured sEMG data set and a specific muscle synergy, which was mostly related to the force generation by the human operator while performing a given task, was searched. Finally, the force and position commands (which were referred to as kinodynamic information) were transferred to a robotic manipulator. The experimental results showed that the pilot human operator was able to successfully perform a given line drawing task by applying various surface pressing forces under our proposed human-robot interface design approach.

Future studies should be followed in the directions of relaxing the over-suppression of transfer gain parameter as well as challenging more complex task with the proposed interface design. Based on findings in this study, we expect that the proposed design approach will be culminated to the development of highly dexterous human-robot interface by which kinodynamic constrained tasks can be successfully performed.

## REFERENCES

- [1] N. Bernstein, *The Co-ordination and Regulation of Movements*. Pergamon Press, 1967.
- [2] L. H. Ting and J. M. Macpherson, "A limited set of muscle synergies for force control during a postural task," *Journal of neurophysiology*, vol. 93, no. 1, pp. 609–613, 2005.
- [3] A. d'Avella and E. Bizzi, "Shared and specific muscle synergies in natural motor behaviors," *Proceedings of the national academy of sciences*, vol. 102, no. 8, pp. 3076–3081, 2005.
- [4] D. J. Berger and A. d'Avella, "Effective force control by muscle synergies," *Frontiers in computational neuroscience*, vol. 8, p. 46, 2014.
- [5] A. Furui, S. Eto, K. Nakagaki, K. Shimada, G. Nakamura, A. Masuda, T. Chin, and T. Tsuji, "A myoelectric prosthetic hand with muscle synergy-based motion determination and impedance model-based biomimetic control," *Science Robotics*, vol. 4, no. 31, p. eaaw6339, 2019.
- [6] A. d'Avella, A. Portone, L. Fernandez, and F. Lacquaniti, "Control of fast-reaching movements by muscle synergy combinations," *Journal of Neuroscience*, vol. 26, no. 30, pp. 7791–7810, 2006.
- [7] J. L. McKay and L. H. Ting, "Functional muscle synergies constrain force production during postural tasks," *Journal of biomechanics*, vol. 41, no. 2, pp. 299–306, 2008.
- [8] K. M. Steele, M. C. Tresch, and E. J. Perreault, "The number and choice of muscles impact the results of muscle synergy analyses," *Frontiers in computational neuroscience*, vol. 7, p. 105, 2013.
- [9] D. Lee and H. S. Seung, "Algorithms for non-negative matrix factorization," *Advances in neural information processing systems*, vol. 13, 2000.
- [10] S. Y. Günay, F. Quivira, and D. Erdoğan, "Muscle synergy-based grasp classification for robotic hand prosthetics," in *Proceedings of the 10th international conference on pervasive technologies related to assistive environments*, pp. 335–338, 2017.
- [11] C. Camardella, M. Barsotti, D. Buongiorno, A. Frisoli, and V. Bevilacqua, "Towards online myoelectric control based on muscle synergies-to-force mapping for robotic applications," *Neurocomputing*, vol. 452, pp. 768–778, 2021.
- [12] S. Chen, J. Yi, and T. Liu, "Muscle synergy-based control of human-manipulator interactions," in *2020 IEEE/ASME International Conference on Advanced Intelligent Mechatronics (AIM)*, pp. 667–672, IEEE, 2020.
- [13] C. G. McDonald, B. J. Fregly, and M. K. O'Malley, "Effect of robotic exoskeleton motion constraints on upper limb muscle synergies: A case study," *IEEE Transactions on Neural Systems and Rehabilitation Engineering*, vol. 29, pp. 2086–2095, 2021.